Generic target response as a measure of regression accuracy in multispectral background estimation

James Theiler
Space Data Science and Systems Group
Los Alamos National Laboratory; Los Alamos, NM 87545, USA
Email: jt@lanl.gov

***Abstract*—This paper introduces a measure of regression fidelity that is directly linked to target detection performance in multispectral and hyperspectral imagery. The measure – called generic target response – maintains this link to target detection without specifying a particular target signature. It is compared to two other measures, one based on variance and one based on volume, in a regression framework that estimates local background from an annular neighborhood. The three generic measures are applied to two hyperspectral images, and are used to compare the performance of three different estimators (local mean, local median, and local linear fit), using two different rotations of the hyperspectral bands.**

***Index Terms*—multispectral imagery, hyperspectral imagery, signal processing, anomaly detection, target detection**

I. Introduction

To detect targets or anomalies in a cluttered scene, one must observe pixels that stand out from the clutter in a statistically significant way, and this requires a quantitative characterization of that background [1]. One way to express the detection problem in imagery is in terms of a hypothesis test at each pixel. The null hypothesis is that the pixel is consistent with a given model of the background; the alternative is that there is a target or anomaly at that pixel. A measure of model quality is the extent to which it enables us to detect targets and anomalies that may be in the scene (without, of course, raising more than a specified number of false alarms).

Usually, when we speak a target, we have in mind a specific target signature $\mathbf{t}$ that corresponds, for instance, to the reflectance spectrum of the material of interest. When we speak of anomalies, we do not have a particular signature in mind, and in general feign ignorance of any properties that an anomaly might possess (except that it is in some unspecified way *unlike* the pixels that make up the background clutter) [2]–[4]. But there is a middle ground, where we do have a target in mind, but its signature $\mathbf{t}$ is variable, perhaps due to variability in the environmental or of its morphological properties (*e.g.*, powder particle size [5]).

Our particular interest here is *point targets*; strictly speaking, these are targets that are smaller than a pixel, but the formalism can be extended to small targets that are a few pixels in spatial extent. For this problem, we can ask – on a pixel-by-pixel basis – what is the expected background distribution.

Some standard detectors (*e.g.*, adaptive matched filter [6]–[9], adaptive coherence estimator [10], finite target matched filter [11], [12]) assume the background is a multivariate Gaussian with a single mean and a single covariance that are both estimated as global properties of the full dataset.

One can often improve this estimate by estimating the mean (and, in some cases, the covariance matrix) locally – *e.g.*, from a segmentation of the image [13], or from a moving window centered on the pixel of interest. The classic RX detector [2] uses an annulus around each pixel to estimate local mean and local covariance, and based on these estimates, computes a Mahalanobis distance as a measure of anomalousness for each pixel. The utility of local estimation for target detection has also been demonstrated [14]–[17].

II. Regression Framework

The problem we consider is the estimation of a vector-valued (*i.e.*, multispectral or hyperspectral) pixel based on the local context of pixels in an annulus around that pixel of interest. What we are estimating here is the target-free value of that pixel; comparison of this target-free value with the actual measured value provides us with a way to assess the competing hypotheses of target-absent versus target-present for that pixel.

For instance, if $\widehat{\mathbf{y}}$ is the estimated (target-absent) value of the pixel, and $\mathbf{y}$ is the measured value, then we can check for an additive target $\mathbf{t}$ with the formula $\mathbf{t}^\intercal R^{-1}(\mathbf{y}-\widehat{\mathbf{y}})$, or for anomalies with $(\mathbf{y}-\widehat{\mathbf{y}})^\intercal R^{-1}(\mathbf{y}-\widehat{\mathbf{y}})$. Here, R is a covariance matrix which may be estimated locally or globally:

$$R = \langle\, (\mathbf{y}-\widehat{\mathbf{y}})(\mathbf{y}-\widehat{\mathbf{y}})^\intercal \,\rangle\,, \tag{1}$$

where $\langle\,\cdot\,\rangle$ indicates an average over pixels, in either the local region of interest or over the whole image. Particularly for local covariance estimation, a regularized estimator [16], [18]–[21] may be preferred over the sample covariance in Eq. (1).

Given an annulus of K pixel values $[\mathbf{x}_1, \ldots, \mathbf{x}_K]$, the aim, as illustrated in Fig. 1, is to find a function of those pixel values that estimates the center pixel: that is,

$$\widehat{\mathbf{y}} = f(\mathbf{x}_1, \ldots, \mathbf{x}_K). \tag{2}$$

A natural choice for this function is simply the average:

$$f(\mathbf{x}_1, \ldots, \mathbf{x}_K) = (\mathbf{x}_1 + \ldots + \mathbf{x}_K)/K. \tag{3}$$

This is the basis for many point-target and anomaly detectors. Since $\widehat{\mathbf{y}}$ is the *distribution mean* of the Gaussian distribution that corresponds to the target-free pixel estimate, then it makes sense to use the *sample mean* in Eq. (3) to estimate it. This would be the right choice (indeed, the optimal choice) if

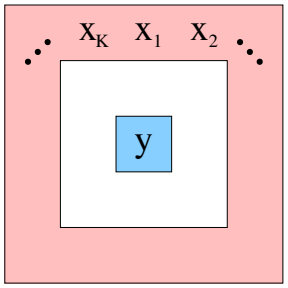

Fig. 1. The central pixel of interest (in blue) has value $\mathbf{y}$. An annulus (in pink) surrounding this pixel has values for K distinct pixels: $\mathbf{x}_1, \mathbf{x}_2, \ldots, \mathbf{x}_K$. The regression framework seeks a function that estimates the central pixels for most pixels in the image: $\mathbf{y} \approx f(\mathbf{x}_1, \ldots, \mathbf{x}_K)$. Those pixels for which the approximation is poor are candidates for locations of targets or anomalies.

there were no local spatial structure; *i.e.*, if $\mathbf{x}_1, \ldots, \mathbf{x}_K$ were independent and identically distributed. But the sample mean is not the only choice, and following earlier work with nested annuli [22], a regression framework has been suggested [23] in which the function f is learned from the data.

III. Generic measures of quality

A. Variance and SNR

A simple way to evaluate how well $\widehat{\mathbf{y}}$ approximates $\mathbf{y}$ is with the mean square difference: $\langle\, (\mathbf{y}-\widehat{\mathbf{y}})^{\mathsf{T}}(\mathbf{y}-\widehat{\mathbf{y}})\,\rangle$. This variance is just the trace of the covariance matrix in Eq. (1); that is:

$$\text{Variance} = \langle\, (\mathbf{y}-\widehat{\mathbf{y}})^{\mathsf{T}}(\mathbf{y}-\widehat{\mathbf{y}})\,\rangle = \text{Trace}(R). \tag{4}$$

One way to compute this quantity in a non-dimensional way is to normalize it by the overall variance of the data: $\langle\, (\mathbf{y}-\boldsymbol{\mu})^{\mathsf{T}}(\mathbf{y}-\boldsymbol{\mu})\,\rangle = \text{Trace}(\widetilde{R})$, where $\boldsymbol{\mu}$ is the *global* mean of $\mathbf{y}$, and $\widetilde{R}$ is the covariance of $\mathbf{y}-\boldsymbol{\mu}$. If we take a negative logarithm of this ratio, we obtain a quality index that is larger for higher quality (*i.e.*, lower variance) estimates:

$$\log\ \text{Variance} = \log \text{Trace}(\widetilde{R}) - \log \text{Trace}(R). \tag{5}$$

An equivalent expression can be obtained in terms of the eigenvalues $(\lambda_1, \ldots, \lambda_d)$ of the $d \times d$ covariance matrix R, and the eigenvalues $(\widetilde{\lambda}_1, \ldots, \widetilde{\lambda}_d)$ of the overall covariance $\widetilde{R}$:

$$\log\ \text{Variance} = \log \sum_i \widetilde{\lambda}_i - \log \sum_i \lambda_i \tag{6}$$

This is related to a signal-to-noise ratio (SNR) and can be expressed in units of decibels:

$$\text{SNR} = \frac{10}{\log 10} \left[\log\ \text{Variance}\right]. \tag{7}$$

B. Log Volume Ratio (LVR)

It was shown in [24] that just because this variance measure is smaller doesn't mean that the target detection performance will be superior, that there are times "when closer isn't better." In [25], this point was acknowledged, and direct measures of performance based on target implantation [26]–[28] were employed to assess the quality of the estimator $\widehat{\mathbf{y}}$. Explicitly implanting targets into an image has the advantage of directness and of unambiguously measuring what we care about – *i.e.*, target detection. But implanting targets is expensive, and often requires making *ad hoc* choices. Another measure of performance was also employed, based on the *volume* of the ellipsoid associated with the covariance matrix of the vectors $\mathbf{y}-\widehat{\mathbf{y}}$, defined in Eq. (1). The use of volume as a proxy for anomaly detection performance was introduced in [29], and employed for a non-ellipsoidal anomaly detector in [30].

Since volume of the ellipsoid is proportional to $|R|$, the determinant of the covariance matrix, which in turn is given by the product of the eigenvalues of R, we can express a log-volume ratio (LVR) measure of estimator quality with

$$\text{LVR} = \log |\widetilde{R}|/|R| = \sum_i \log \widetilde{\lambda}_i - \sum_i \log \lambda_i. \tag{8}$$

C. Generic target response (GTR)

This discussion introduces a third measure of fitness quality that is directly related to how well a matched filter would perform in detecting an additive target $\mathbf{t}$. This target response measure will then be extended to a *generic target response* measure that is not tied to a specific target signature.

For an additive target on a Gaussian background, the adaptive matched filter is the optimal detector [6]–[8]. The detector for target $\mathbf{t}$, given local estimate $\widehat{\mathbf{y}}$ and covariance R, is:

$$\mathcal{D}(\mathbf{y}) = \mathbf{t}^{\mathsf{T}} R^{-1}(\mathbf{y}-\widehat{\mathbf{y}}). \tag{9}$$

We expect $\mathcal{D}(\mathbf{y})$ to be large if the pixel measurement $\mathbf{y}$ includes the target $\mathbf{t}$, and to be small if there is no target. Over non-target (background) pixels, $\mathcal{D}(\mathbf{y})$ has mean $\mu_n = 0$ and variance $\sigma_n^2 = \mathbf{t}^{\mathsf{T}} R^{-1}\mathbf{t}$; for an average pixel *with* additive target $\mathbf{t}$, the expected response $\mathcal{D}(\mathbf{y})$ is $\mu_t = \mathbf{t}^{\mathsf{T}} R^{-1}\mathbf{t}$. Informally, this is $(\mu_t - \mu_n)/\sigma_n = \sqrt{\mathbf{t}^{\mathsf{T}} R^{-1}\mathbf{t}}$ "sigmas" of significance. The better $\widehat{\mathbf{y}}$ approximates $\mathbf{y}$, the "smaller" R will be, and the larger R^{-1} and therefore $\mathbf{t}^T R^{-1}\mathbf{t}$ will be; thus a better estimator for $\widehat{y}$ corresponds to a more significant detection, on average, of a target $\mathbf{t}$. And the appropriate measure of quality for the fit of $\widehat{\mathbf{y}}$ to $\mathbf{y}$ is thus given by

$$\begin{aligned}\mathbf{t}^{\mathsf{T}} R^{-1}\mathbf{t} &= \text{Trace}\left(\mathbf{t}^{\mathsf{T}} R^{-1}\mathbf{t}\right) = \text{Trace}\left(R^{-1}\mathbf{t}\mathbf{t}^{\mathsf{T}}\right) \\ &= \sum_i \lambda_i^{-1}\mathbf{u}_i^{\mathsf{T}}(\mathbf{t}\mathbf{t}^{\mathsf{T}})\mathbf{u}_i = \sum_i \lambda_i^{-1} v_i^2,\end{aligned} \tag{10}$$

where $\mathbf{u}_i$ is the ith eigenvector of R, associated with the eigenvalue λ_i, and v_i^2 is the variance in the direction $\mathbf{u}_i$ associated with the target matrix $\mathbf{t}\mathbf{t}^{\mathsf{T}}$. In particular, $v_i = \mathbf{u}_i^{\mathsf{T}}\mathbf{t}$.

While Eq. (10) provides a measure appropriate to a specific target, we can produce a *generic* target response by averaging this response over a distribution of targets. In particular, if $p(\mathbf{t})$ is a probability density function for an ensemble of potential targets, then the expected value of the target response is given by

$$\begin{aligned}\int \text{Trace}\left(R^{-1}\mathbf{t}\mathbf{t}^{\mathsf{T}}\right) p(\mathbf{t})d\mathbf{t} &= \text{Trace}\left(R^{-1}\int \mathbf{t}\mathbf{t}^{\mathsf{T}} p(\mathbf{t})d\mathbf{t}\right) \\ &= \text{Trace}\left(R^{-1}\left\langle\, \mathbf{t}\mathbf{t}^{\mathsf{T}}\,\right\rangle\right).\end{aligned} \tag{11}$$

Arguably the "most" generic target is one whose direction is isotropic; that is $\langle\, \mathbf{t}\mathbf{t}^{\mathsf{T}}\,\rangle = I$. This leads to an alternative to

TABLE I

GENERIC MEASURES OF REGRESSION QUALITY (LARGER VALUES ARE HIGHER QUALITY). HERE R IS THE COVARIANCE MATRIX DEFINED IN EQ. (1), AND λ_i IS THE iTH EIGENVALUE OF R. GTR CORRESPONDS TO GENERIC TARGET RESPONSE.

Measure	Matrix formulation	Eigenvalue formulation
log Variance	$-\log \text{Trace}(R)$	$-\log \sum_i \lambda_i$
log Volume	$-\log \lvert R \rvert$	$-\sum_i \log \lambda_i$
log Volume	$\log \lvert R^{-1} \rvert$	$\sum_i \log \lambda_i^{-1}$
Isotropic GTR	$\log \text{Trace}(R^{-1})$	$\log \sum_i \lambda_i^{-1}$
Generalized GTR′	$\log \text{Trace}(R^{-1} \langle \mathbf{t}\mathbf{t}^\mathsf{T} \rangle)$	$\log \sum_i \lambda_i^{-1} v_i^2$

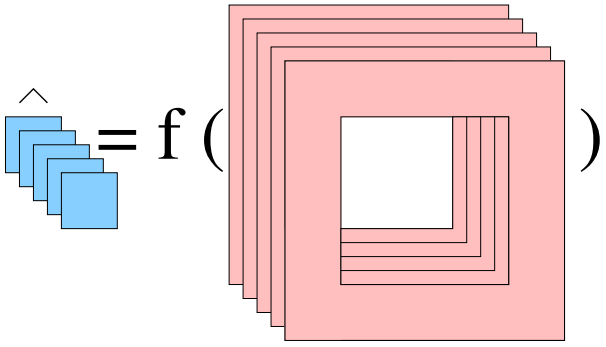

Fig. 2. The aim of local background modeling is to estimate a multi-band pixel value (illustrated in blue) as a function of the multi-band pixels in the annulus (illustrated in pink) that surround the pixel of interest.

Eq. (7) and Eq. (8), one that is similarly generic, but that is particularly associated with target detection. Our generic target response criterion is:

$$\text{GTR} = \log \text{Trace}(R^{-1}) - \log \text{Trace}(\widetilde{R}^{-1}) \tag{12}$$

$$= \log \sum_i \lambda_i^{-1} - \log \sum_i \widetilde{\lambda}_i^{-1}. \tag{13}$$

We can generalize this expression to non-isotropic, but still fairly generic distributions on $\mathbf{t}$, characterized by the target matrix $\langle \mathbf{t}\mathbf{t}^\mathsf{T} \rangle$. If $v_i^2 = \mathbf{u}_i^\mathsf{T} \langle \mathbf{t}\mathbf{t}^\mathsf{T} \rangle \mathbf{u}_i$ is the variance of the target matrix in the direction of the ith eigenvector $\mathbf{u}_i$ of R, then

$$\text{GTR}' = \log \sum_i \lambda_i^{-1} v_i^2 - \log \sum_i \widetilde{\lambda}_i^{-1} v_i^2. \tag{14}$$

Table I shows how the formulas for the three generic measures (in un-normalized form) are related to each other.

IV. APPLICATION TO MULTI-BAND IMAGERY

In applying Eq. (2) to imagery with d spectral bands, the problem that is illustrated in Fig. 2, we have several options. The most general treats each $\mathbf{x}_k$ as the vector of radiances or reflectances associated with each band of pixel k. There are effectively Kd scalar arguments for the function f in this case. Since the output of f is vector-valued with d components, a linear function f would have Kd^2 coefficients.

A subset of these options considers band-by-band modeling. Here, a separate function f is computed for each band, based on surrounding pixels that are in the same band. Each function f has only K scalar arguments, and produces a single scalar output. If these are all linear models, then there are a total of Kd distinct coefficients, since there are d separate functions that are fit to the data.

Two kinds of band-by-band modeling will be considered. Direct band-by-band modeling is straightforward, it simply treats each band separately; but this direct approach fails to take account of the correlations between bands. Principal components analysis (PCA) band-by-band modeling attempts to (at least partially) account for these correlations without introducing cross-band coefficients by performing PCA on the image, and then treating each principal component band separately.

Table II(a) lists the generic measures of background estimation quality (SNR, LVR, and GTR) for the 128-band HyMap Cooke City dataset [31]. Here the annulus is a 5×5 patch with the center pixel missing (thus $K = 24$ pixels in the annulus) and it is applied both in the direct band-by-band mode and with PCA band-by-band. Three estimators are employed: the mean is given by Eq. (3), the median takes the median of the 24 pixel values, and a linear model

$$f(x_1, \ldots, x_K) = a_1 x_1 + \ldots + a_k x_K \tag{15}$$

is fit to each band.

The same experiment is applied to a different data set, the 200-band AVIRIS Indian Pines dataset [32], and the results are shown in Table II(b).

V. CONCLUSIONS

One of the key conclusions, in terms of background modeling, is that linear regression substantially outperforms mean and median. This shows that local spatial structure, which mean and median ignore, *can* be usefully exploited by the background model. This is evident in all three measures of estimation accuracy (the regression model is closer *and* better), and for both PCA and direct band-by-band modeling.

We also observe that the LVR and GTR scores are generally higher for PCA than direct band-by-band modeling. This tells us that the PCA modeling is more effective, which can be interpreted in terms of *spectral* correlations being usefully exploited. However, this improvement is *not* evident from the SNR measure, which confirms the inadequacy of SNR that was pointed out in [24]. (This distinction is also not evident with the mean estimator in Eq. (3), since the mean estimate is the same for direct and PCA.) A third observation is that mean generally outperforms median, though the difference is more striking in the direct band-by-band case.

Although SNR is an intuitively plausible choice for measuring the accuracy of regression models, we see that it lacks the sensitivity to compare competing approaches for background estimation. The LVR was motivated by anomaly detection problems [29], [30], [33], but the GTR introduced here is specifically designed to measure target detection performance,

Fig. 3. Bands 3, 5, and 15 of the 128-band hyperspectral image of Cooke City, Montana, are combined into blue, green, and red channels, respectively, of this color image.

TABLE II
MEASURES OF QUALITY FOR THREE REGRESSION FUNCTIONS f, APPLIED TO TWO HYPERSPECTRAL IMAGES.

(a) 128-band Cooke City hyperspectral image [31]

	PCA band-by-band			direct band-by-band		
$f(\mathbf{x}_1, \ldots, \mathbf{x}_K)$	SNR	LVR	GTR	SNR	LVR	GTR
Median	12.5	98.1	0.49	12.5	3.1	-0.23
Mean	12.1	99.8	0.50	12.1	99.8	0.50
Linear	25.5	300.7	1.70	25.5	287.0	1.56

(b) 200-band Indian Pines hyperspectral image [32]

	PCA band-by-band			direct band-by-band		
$f(\mathbf{x}_1, \ldots, \mathbf{x}_K)$	SNR	LVR	GTR	SNR	LVR	GTR
Median	9.2	17.4	0.01	9.2	-21.0	-0.14
Mean	8.6	20.9	0.03	8.6	20.9	0.03
Linear	17.1	101.0	0.54	16.6	56.7	0.37

but for non-specific targets. A potential advantage of GTR is that its generalization, shown in Eq. (14), enables a more flexible and quantitative way to address target variability.

ACKNOWLEDGMENTS

This work was supported by the United States Department of Energy (DOE) NA-22 Hyperspectral Advanced Research and Development (HARD) Solids project. I am grateful to Brendt Wohlberg and Stanley Rotman for valuable discussions.

REFERENCES

[1] S. Matteoli, M. Diani, and J. Theiler, "An overview background modeling for detection of targets and anomalies in hyperspectral remotely sensed imagery," *IEEE J. Sel. Topics in Applied Earth Observations and Remote Sensing*, vol. 7, pp. 2317–2336, 2014.

[2] I. S. Reed and X. Yu, "Adaptive multiple-band CFAR detection of an optical pattern with unknown spectral distribution," *IEEE Trans. Acoustics, Speech, and Signal Processing*, vol. 38, pp. 1760–1770, 1990.

[3] S. Matteoli, M. Diani, and G. Corsini, "A tutorial overview of anomaly detection in hyperspectral images," *IEEE A&E Systems Magazine*, vol. 25, pp. 5–27, 2010.

[4] J. Theiler, "By definition undefined: Adventures in anomaly (and anomalous change) detection," *Proc. 6th IEEE Workshop on Hyperspectral Image and Signal Processing: Evolution in Remote Sensing (WHISPERS)*, 2014.

[5] T. L. Myers, C. S. Brauer, Y.-F. Su, T. A. Blake, R. G. Tonkyn, A. B. Ertel, T. J. Johnson, and R. L. Richardson, "Quantitative reflectance spectra of solid powders as a function of particle size," *Applied Optics*, vol. 54, pp. 4863–4875, 2015.

[6] I. S. Reed, J. D. Mallett, and L. E. Brennan, "Rapid convergence rate in adaptive arrays," *IEEE Trans. Aerospace and Electronic Systems*, vol. 10, pp. 853–863, 1974.

[7] E. J. Kelly, "An adaptive detection algorithm," *IEEE Trans. Aerospace and Electronic Systems*, vol. 22, pp. 115–127, 1986.

[8] F. C. Robey, D. R. Fuhrmann, E. J. Kelly, and R. Nitzberg, "A CFAR adaptive matched filter detector," *IEEE Trans. Aerospace and Electronic Systems*, vol. 28, pp. 208–216, 1992.

[9] B. R. Foy, J. Theiler, and A. M. Fraser, "Unreasonable effectiveness of the adaptive matched filter," *Proc. MSS (Military Sensing Symposia) Passive Sensors Conference*, 2006.

[10] S. Kraut, L. L. Scharf, and R. W. Butler, "The Adaptive Coherence Estimator: a uniformly most-powerful-invariant adaptive detection statistic," *IEEE Trans. Signal Processing*, vol. 53, pp. 427–438, 2005.

[11] A. Schaum and A. Stocker, "Spectrally selective target detection," *Proc. ISSSR (International Symposium on Spectral Sensing Research)*, p. 23, 1997.

[12] B. R. Foy, J. Theiler, and A. M. Fraser, "Decision boundaries in two dimensions for target detection in hyperspectral imagery," vol. 17, pp. 17391–17411, 2009.

[13] J. Theiler and L. Prasad, "Overlapping image segmentation for context-dependent anomaly detection," *Proc. SPIE*, vol. 8048, pp. 804807, 2011.

[14] Y. Cohen and S. R. Rotman, "Spatial-spectral filtering for the detection of point targets in multi- and hyperspectral data," *Proc. SPIE*, vol. 5806, pp. 47–55, 2005.

[15] C. E. Caefer, M. S. Stefanou, E. D. Nelson, A. P. Rizzuto, O. Raviv, and S. R. Rotman, "Analysis of false alarm distributions in the development and evaluation of hyperspectral point target detection algorithms," *Optical Engineering*, vol. 46, pp. 076402, 2007.

[16] C. E. Caefer, J. Silverman, O. Orthal, D. Antonelli, Y. Sharoni, and S. R. Rotman, "Improved covariance matrices for point target detection in hyperspectral data," *Optical Engineering*, vol. 47, pp. 076402, 2008.

[17] Y. Cohen, D. G. Blumberg, and S. R. Rotman, "Subpixel hyperspectral target detection using local spectral and spatial information," *J. Applied Remote Sensing*, vol. 6, pp. 063508, 2012.

[18] J. P. Hoffbeck and D. A. Landgrebe, "Covariance matrix estimation and classification with limited training data," *IEEE Trans. Pattern Analysis and Machine Intelligence*, vol. 18, pp. 763–767, 1996.

[19] G. Cao and C. A. Bouman, "Covariance estimation for high dimensional data vectors using the sparse matrix transform," *Advances in Neural Information Processing Systems*, vol. 21, pp. 225–232, 2009.

[20] J. Theiler, "The incredible shrinking covariance estimator," *Proc. SPIE*, vol. 8391, pp. 83910P, 2012.

[21] L. Bachega, J. Theiler, and C. A. Bouman, "Evaluating and improving local hyperspectral anomaly detectors," *IEEE Applied Imagery and Pattern Recognition (AIPR) Workshop*, vol. 39, 2011.

[22] J. Theiler and J. Bloch, "Multiple concentric annuli for characterizing spatially nonuniform backgrounds," *The Astrophysical Journal*, vol. 519, pp. 372–388, 1999.

[23] J. Theiler and B. Wohlberg, "Regression framework for background estimation in remote sensing imagery," *Proc. 5th IEEE Workshop on Hyperspectral Image and Signal Processing: Evolution in Remote Sensing (WHISPERS)*, 2013.

[24] N. Hasson, S. Asulin, S. R. Rotman, and D. Blumberg, "Evaluating backgrounds for subpixel target detection: when closer isn't better," *Proc. SPIE*, vol. 9472, pp. 94720R, 2015.

[25] J. Theiler, "Symmetrized regression for hyperspectral background estimation," *Proc. SPIE*, vol. 9472, pp. 94721G, 2015.

[26] W. F. Basener, E. Nance, and J. Kerekes, "The target implant method for predicting target difficulty and detector performance in hyperspectral imagery," *Proc. SPIE*, vol. 8048, pp. 80481H, 2011.

[27] Y. Cohen, Y. August, D. G. Blumberg, and S. R. Rotman, "Evaluating sub-pixel target detection algorithms in hyper-spectral imagery," *J. Electrical and Computer Engineering*, vol. 2012, pp. 103286, 2012.

[28] J. Theiler, "Matched-pair machine learning," *Technometrics*, vol. 55, pp. 536–547, 2013.

[29] J. Theiler and D. Hush, "Statistics for characterizing data on the periphery," *Proc. IEEE Int. Geoscience and Remote Sensing Symposium (IGARSS)*, pp. 4764–4767, 2010.

[30] J. Theiler, "Ellipsoid-simplex hybrid for hyperspectral anomaly detection," *Proc. 3rd IEEE Workshop on Hyperspectral Image and Signal Processing: Evolution in Remote Sensing (WHISPERS)*, 2011.

[31] D. Snyder, J. Kerekes, I. Fairweather, R. Crabtree, J. Shive, and S. Hager, "Development of a web-based application to evaluate target finding algorithms," *Proc. IEEE International Geoscience and Remote Sensing Symposium (IGARSS)*, vol. 2, pp. 915–918, 2008.

[32] D. A. Landgrebe, *Signal Theory Methods in Multispectral Remote Sensing*, John Wiley & Sons, 2003.

[33] G. Grosklos and J. Theiler, "Ellipsoids for anomaly detection in remote sensing imagery," *Proc. SPIE*, vol. 9472, pp. 94720P, 2015.